J Porous Mater (2018) 25:945–953
DOI 10.1007/s10934-017-0506-y

Saponin-loaded SBA-15: release properties and cytotoxicity to Panc-I cancer cells

Suman Jangra[1,2] · Bharti Sharma[3] · Rahul Jangra[2] · Vinod Chhokar[2] · Surender Duhan[1]

Published online: 16 September 2017

Abstract In this study, first time a nanoformulation, saponin-loaded SBA-15 has been developed for an improved and continuous release. The SBA-15 nanopowder was synthesized by a hydrothermal process. Saponin was introduced into the mesoporous channels of SBA-15 and its concentration in SBA-15 was measured by UV–visible spectrophotometry. The pristine SBA-15 and saponin-loaded SBA-15 were characterized by small-angle XRD, FESEM, HRTEM, TGA, FTIR. N_2 adsorption–desorption isotherms were used to measure the specific surface area and pore channel structure parameters of pristine and loaded SBA-15. Saponin release was studied in phosphate buffered saline (pH 7.4), which revealed that the release rate could be effectively controlled. The controlled drug release is highly desired for cancer treatment. The cytotoxicity of pristine and loaded SBA-15 was analyzed on Panc-I cancer cells. Both the pristine SBA-15 and saponin-loaded SBA-15 nanoparticles showed specific toxicity on the cancer cells. The preliminary results showed that saponin-loaded SBA-15 could be an effective therapeutic agent for Panc-I cancer cells.

Keywords Mesoporous silica · Controlled release · Saponin · Cytotoxicity · Cancer cell

✉ Suman Jangra
jangraguddu2007@gmail.com

[1] Nanomaterials Research Laboratory, Department of Materials Science & Nanotechnology, D. C. R. University of Science & Technology, Murthal, Sonepat 131039, India

[2] Proteomics and Genomics Research Laboratory, Department of Bio & Nanotechnology, G.J. University of Science & Technology, Hisar, Haryana 125001, India

[3] Department of Physics and Astrophysics, University of Delhi, Delhi 110007, India

1 Introduction

Saponins are naturally occurring large family of amphiphilic compounds widely distributed in higher plants and commonly found in leaves, roots, tubers, blooms or seeds [1]. Saponins can be categorized into triterpenes and steroids on the basis of the carbon skeletons. The glycone part of saponinis generally oligosaccharide, organized in a linear or branched manner and through an acetal linkage attached to hydroxyl groups [2]. Saponins are non-toxic to humans upon oral intake. However, when the sponins injected into the bloodstream, they can act as powerful hemolytic agents [3]. Saponins are also act as lipase inhibitors [3]. Some sanitized portions of Quilla jasaponaria have adjuvant activity [4, 5]. Some important properties of saponins include generation of molecular compounds with cholesterol as well as other hydroxyl steroids, ability to generate foam when mixed in aqueous solutions, generation of emulsions with oils, toxicity to amphibians and fish [6, 7]. Current research on saponins revealed their anti-tumor effect on various cancer cells [1]. Several saponins prevent tumor cell growth through cell cycle arrest [1]. Furthermore, the use of saponins with well-known tumor treatment strategies presents improved therapeutic effect. Saponin has interesting biological activities such as hypo cholesterolaemic, anti-tumorigenic, immune-stimulatory effects [3]. However, the wide spectrum action of saponins in the medical field is limited by their insolubility [3].

Over the past couple of decades, nanosuspension technology has gained significant attention of research society in pharmaceutics since the poor water-solubility of new chemical entities and difficulty to formulate via conventional techniques [8, 9]. The nanosuspensions consist of a liquid colloidal dispersion in nanoscale (10–1000 nm) and surfactants or polymers as stabilizers [10]. The nanosuspensions are very

effective in improving the dissolution rate and especially, the oral bioavailability of poorly water soluble drugs [11, 12]. However, modern research is focused on poorly soluble controlled drug delivery vehicles like ordered mesoporous silicas: AMS-1, SBA-15 and SBA-16 [13, 14]. The SBA-15 is a favorable drug carrier due to its various beneficial properties such as stable arranged mesoporous structure, very large specific surface area, tunable pore size, large pore volume and outstanding biocompatibility [15–17]. Additionally, the adsorption ability of poorly soluble drugs onto the surface of SBA-15 is an emerging tactic for enhancing drug dissolution [18]. Nano sized drug delivery carrier such as SBA-15 can be an evolving tactic for saponin delivery and tumor targeting [19].

In the present study, first time the release properties and cytotoxicity to cancer cell lines of saponin loaded SBA-15 are described in detail. The proposed controlled release system has an inordinate potential to achieve a sustained release of poorly water-soluble saponin.

2 Materials and methods

2.1 Materials

Ethylene oxide–propylene oxide–ethylene oxide ($EO_{20}PO_{70}EO_{20}$, Pluronic P_{123}) with molecular weight, Mw = 5800, tetraethoxyorthosilicate [$(C_2H_5O)_4Si$, TEOS], Hydrochloric acid, HCl (35%) and saponin from quillaja bark purified were procured from Sigma-Aldrich, India. Double deionized water was used. All chemicals and solvents were of analytical grade.

2.2 Synthesis of pure SBA-15 matrix

Mesoporous silica, SBA-15 was synthesized according to our earlier reported works [15–17]. At first 2 g of P_{123} was dissolved in 70 ml double distilled water at 40 °C in high acidic conditions achieved by the addition of 10 ml HCl (2 M). Then, a clear solution was obtained approximately after 3 h of uninterrupted magnetic stirring. After that 4.8 ml TEOS was slowly added to the obtained solution under uninterrupted magnetic stirring for 24 h at 40 °C. Subsequently, the resulting solution was moved to a stainless steel autoclave for hydrothermal treatment at 100 °C for 24 h. At ambient temperature (~28 °C), the solid material was filtered, washed and allowed to dry at 70 °C in a hot air oven. At last, the solid material was calcined in a furnace at 600 °C for 4 h with a constant heating rate of 1 °C/min to eliminate organic templates. The finally obtained white powder is pure mesoporous silica, SBA-15.

2.3 Saponin loading

Initially 200 mg of the support was soaked in 50 mL of saponin-ethanol solution (0.5 mg mL^{-1}) and constantly stirred for 24 h at room temperature avoiding solvent evaporation. The saponin loaded sample was first filtered and then dried again at room temperature. Afterwards, the filtrate (1.0 mL) was properly diluted in ethanol to estimate the concentration of saponin using a UV–Vis spectrophotometer at 428 nm. The loading concentration of saponin was estimated using Eq. (1).

$$P_E = \frac{C_i - C_f}{W} \times V \tag{1}$$

where, P_E is loading concentration of saponin absorbed into the mesoporous matrix (mg g^{-1}, mg saponin per gram SBA-15), while C_i and C_f are initial and final concentrations of the saponin in the solution (mg mL^{-1}) respectively. W is weight of the SBA-15 (g) and V is volume of the solution (mL).

2.4 Saponin release

In vitro saponin release from the SBA-15 was accomplished as follows: at first, 40 mg of the sample was absorbed in 50 mL of phosphate buffer (PBS), pH 7.4 with gentle stirring at 37 °C. Subsequently, 5 mL of the solution was removed at predefined time interval and immediately replaced by 5 mL of new PBS. The removed 5 mL solution was filtered and scrutinized by UV–Vis spectrophotometer. As some share of the saponin loaded sample was removed from the release mixture, therefore that portion of the saponin cannot be counted for next sampling. So, a corrected method [20] was used to estimate the real concentration of the released saponin using Eq. (2).

$$C_{t\text{-}corrected} = C_t + \frac{v}{V}\sum_{0}^{t-1} C_t \tag{2}$$

where, $C_{t\text{-}corrected}$ (mg mL^{-1}) is the actual content of saponin released at time t, C_t is concentration of release fluid determined by UV–visible spectrometer (mg mL^{-1}) sampled at time t, v is sampled volume reserved at particular time interval (mL), and V is total volume of released fluid (mL).

The real quantity of saponin released from SBA-15 in the release fluid was calculated using Eq. (3).

$$A_{t\text{-}released} = \frac{C_{t-corrected} \times V}{P_E} \times 100 \tag{3}$$

where $A_{t\text{-released}}$ is the real quantity of released saponin at time t (%), $C_{t\text{-corrected}}$ is the concentration of released saponin at time t, V is total volume of release fluid, and P_E is loading

concentration of the saponin absorbed into the mesoporous matrix.

2.5 Cytotoxicity measurement

For cytotoxicity measurement Panc-I cells were seeded on 96 well plate with a high density (10^4 cells per well). MTT (3-(4,5-dimethylthiazole-2-yl)-2,5-diphenyl tetrazolium bromide) assay [3] was used to measure cytotoxicity of SBA-15 nanoparticles. The measurement was a colorimetric test centered on selective capacity of viable cells to diminish the tetrazolium part of MTT into a purple colored formazan crystal. The concentration of about 1 mg/ml of SBA-15 was taken by dilution with the media. Five different concentrations of saponin such as 0.25, 0.50, 1, 2, 5 µg/ml were taken for the measurement. After achieving 90% confluency, the cells were cleaned with PBS buffer and different content of nanoparticles were incorporated and incubated. Pristine cells in media acted as a negative control and wells treated with a nonionic surfactant, Triton X-100 acted as a positive control for 24 h. About 5 mg of MTT was diluted in 1 ml of PBS. Thereafter, 10 µl of the MTT solution was furthermore diluted to 100 µl with a 90 µl of serum-free phenol red medium. Later on, the cells were incubated for 4 h to generate formazan crystals. The absorbance was characterized at 580 nm by a spectrophotometer (ELISA plate reader).

2.6 Cell culture

Dulbecco's modified Eagle's medium supplemented with 10% fetal bovine serum and 1% penicillin/streptomycin was used to grow Panc-I cells. Cell suspensions were added to 25 cm^2 vials and moved to an incubator at 37 °C in presence of 5% CO_2. Afterwards, the cells were trypsinized using 1% trypsin solution and collected from the bottom of 25 cm^2 vials when the cells are in a semi-confluent state or in log phase of growth. For examining the cell feasibility with nanoparticles, the cell was trypsinized and resuspended in fresh media, 24 h prior to the treatment, 100,000 cells per 1 mL fresh media were added to each well of a sanitized 24-well plate, and moved to the incubator for attachment and instantaneous overnight growth. Then on next day, three different dosages of the samples were added to the cells at a confluency of 70–80% and spin mixed, transferred back to the incubator. After 3 days of growth, the plate is taken out, and the cells in each well were washed three times with sterile PBS.

2.7 Characterization

The concentration of saponin in saponin-loaded SBA-15 was estimated by UV–visible spectrophotometry (Shimadzu UV-2450, Milton Keynes, UK) according to Eq. (1) [21]. Small-angle X-ray diffraction (XRD) was performed using a Bruker D8 advance diffractometer with Cu-Kα target (λ = 0.15418 nm) to characterize the crystallinity of the samples. The XRD spectra was recorded from 0.5° to 4° with a scanning step of 0.01° and time per step of 10 s. Field emission scanning electron microscope (FESEM, FEI QUANTA 200F) and high resolution transmission electron microscope (HRTEM, TECNAI G20) were used to characterize the morphology of samples. Thermo-gravimetric analysis (TGA) was performed using a SDT Instrument (Q-600 DSC–TGA). Thermograms were recorded from 30 to 800 °C at a uniform heating rate of 10 °C/min with nitrogen (N_2) purge gas. Fourier transform infrared (FTIR) spectra of samples were recorded on a Perkin-Elmer BX II spectrophotometer with potassium bromide (KBr), in the range of 4000–400 cm^{-1}. At very low temperature of −196 °C, nitrogen (N_2) adsorption–desorption isotherms were recorded using a Micrometrics Tri-Star analyzer. N_2 adsorption–desorption isotherms were used to determine the specific surface area and pore channel structure parameters by following BET (Brunner–Emmett–Teller) method [22]. The pore volume and pore size distribution were measured by following Barrett–Joyner–Halenda (BJH) model [23].

3 Results and discussion

3.1 Small angle X-ray diffraction

Small angle XRD pattern of SBA-15 and saponin-loaded SBA-15 are shown in Fig. 1. The typical XRD pattern of mesoporous SBA-15 shows a strong diffraction peak attributed to (100) plane with d-spacing value of 93.1 Å. The XRD pattern also reveals two quite weak but resolved

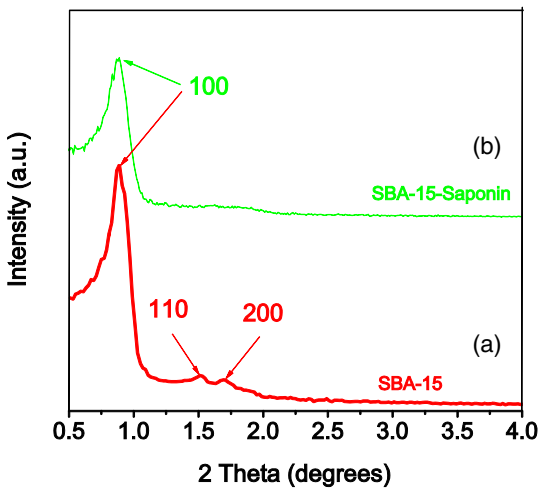

Fig. 1 Small angle XRD patterns of (a) SBA-15 and (b) saponin-loaded SBA-15

peaks attributing to (110) and (200) planes. These two well resolved weak peaks reflected by small angle XRD pattern are due to the characteristics of hexagonal arranged mesoporous structure of SBA-15 [24]. All three peaks at 0.9°, 1.52° and 1.7° respectively confirms a highly ordered with p6mm hexagonal symmetric structure of SBA-15. The characteristic peaks of mesoporous SBA-15 are in close agreement with the literature [25]. However, the small angle XRD pattern of saponin-loaded SBA-15 shows a noticeable decrease in intensity of the diffraction peaks and a slight increase in d-spacing value (99.3 Å). The decrease in intensity of diffraction peaks may be due to the filling of pores of mesoporous structure of SBA-15, which can diminish the scattering disparity between the pores and their side walls of SBA-15 [26, 27].

3.2 FESEM analysis

FESEM images of SBA-15 and saponin-loaded SBA-15 at relatively low and high magnifications are shown in Fig. 2. The FESEM micrographs (Fig. 2a, b) reveals somewhat rod-like domains aggregated to wheat-like structures. Such type of structures generally consists of large fibrous structures ranging from 0.5 to 1 µm in diameter and from 3 to 6 µm in length, as designated by dotted white circle (Fig. 2b). The fibrous structures are the group of huge quantity of fibers generally made of small rod type particles of diameter 0.1–0.3 µm and length 0.1–2 µm [28], as indicated by solid white circle (Fig. 2b). The FESEM micrographs also reveal weakly trapezoidal shape wheat grain type particles. This happens due to the involvement of various synthesis parameters of SBA-15 such as temperature, electrolytes, co-surfactants, pH, and swelling agents, etc. [25]. The low magnification micrograph of saponin-loaded SBA-15 (Fig. 2c) seems almost similar to that of the SBA-15 (Fig. 2a). However, at high magnification, a clear difference in the morphology of both the materials can be easily observed. The FESEM micrograph of saponin-loaded SBA-15 also reveals rod-like packed domains agglomerated to wheat-like structures, as designated by dotted white circle (Fig. 2d). But, the diameter as well as the length of these domains appears larger than the domains seen in case of SBA-15. On the other hand, the micrographs of saponin-loaded SBA-15 display integrated small rod units with tightly packed macrostructures of amorphous units, as indicated by solid white

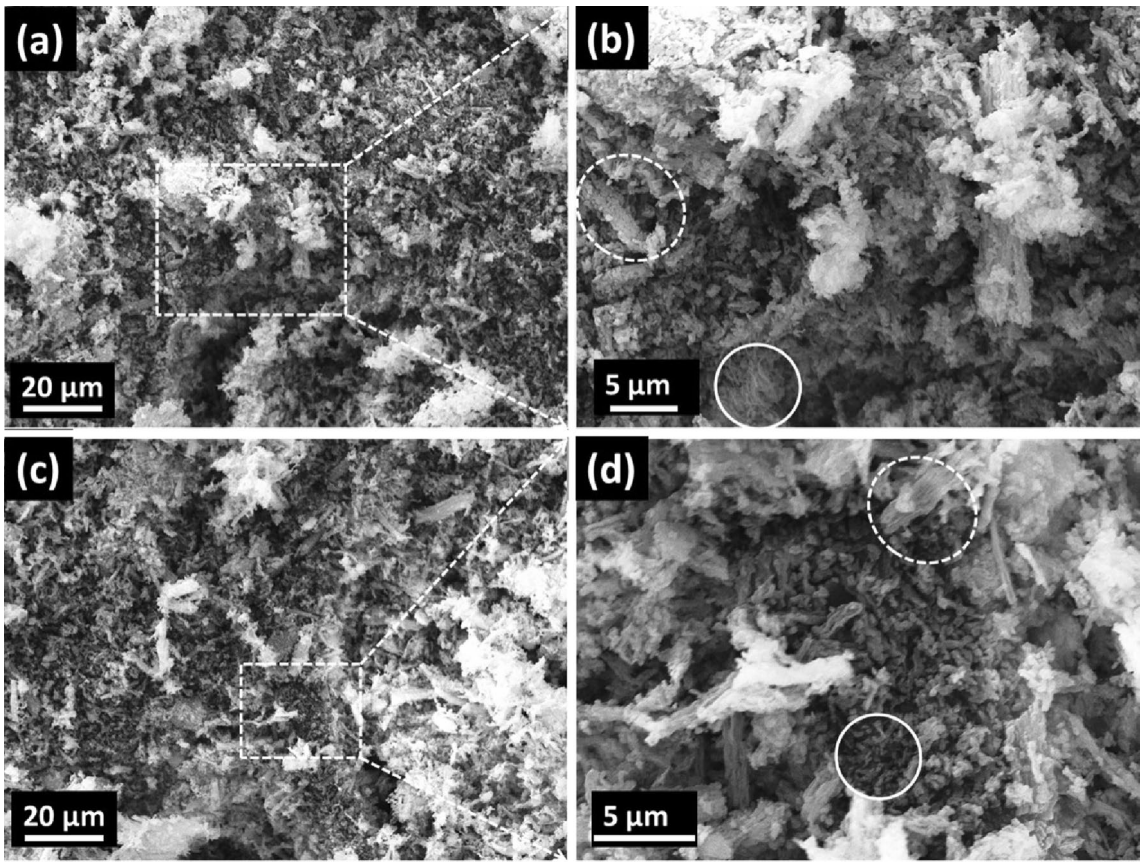

Fig. 2 FESEM images of **a, b** SBA-15 and **c, d** saponin-loaded SBA-15

circle (Fig. 2d). The significantly modified morphology is because of the loading of saponin in SBA-15.

3.3 HRTEM analysis

HRTEM micrograph of SBA-15 (Fig. 3a) reveals the ordered structure with cylindrical nano-pores well-organized in a hexagonal array. This type of structure is found in close agreement with the structure estimated from the small-angle XRD pattern of SBA-15 (Fig. 1). Figure 3a shows the 2-dimensional (2D) hexagonal, p6mm structure consisting identical cylindrical pores of same width to efficiently accommodate saponin. The mesochannels in rod type of particles are along the long axis [28]. The diameter of mesochannels in SBA-15 is very small even less than 10 nm. It is also realized that the nano-pores are not connected with each other. The entrapment of saponin into the mesochannels of SBA-15 does not affect its hexagonal arranged structure (Fig. 3b). However, the HRTEM micrograph of saponin-loaded SBA-15 does not reveal any existence of agglomerated saponin particles that may be due to the homogeneous distribution of saponin into the pores of mesochannels of SBA-15 [15].

3.4 Thermal analysis

Thermal stability of prepared samples was investigated using TGA curves. The TGA thermograms of SBA-15, saponin and saponin-loaded SBA-15 are shown in Fig. 4. The thermogram of SBA-15 indicates a small mass loss about 8.9% up to 800 °C. A minimal mass loss of SBA-15 up to 200 °C ascribed to thermo-desorption of water from mesopores of SBA-15. After that no significant mass loss was observed on heating SBA-15 to 800 °C. However, a small mass loss of SBA-15 from 650 to 800 °C is ascribed to the condensation and dehydroxylation of silanol groups [15]. The TGA profile of saponin shows a significant mass loss at 300 °C. The saponin alone shows a sharp degradation at 300 °C, which

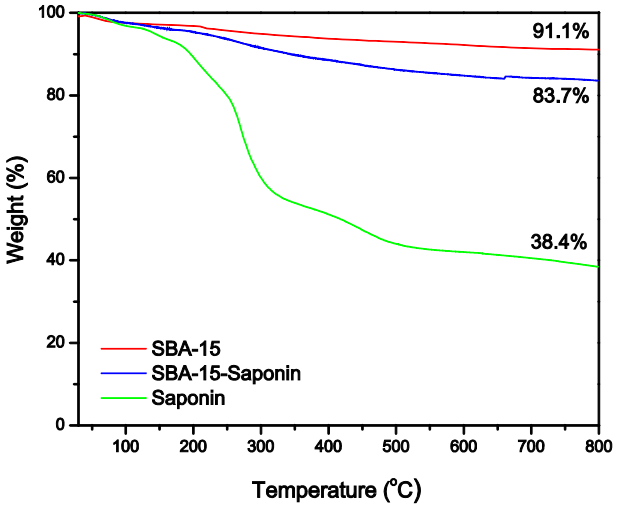

Fig. 4 TGA thermograms of SBA-15, saponin and saponin-loaded SBA-15

point out that the melting point of saponin lies somewhere at this temperature range. At 800 °C, the saponin loses its significant mass about 61.6%. Conversely, the saponin-loaded SBA-15 shows a better stability throughout the temperature range even at 800 °C with 83.7% remnant. The initial mass loss of saponin-loaded SBA-15 by heating up to 250 °C corresponds to solvent removal. The mass loss observed from 250 to 800 °C corresponds to the decomposition of saponin.

3.5 FTIR studies

Fourier transform infrared (FTIR) spectra of SBA-15, saponin and saponin-loaded SBA-15 are shown in Fig. 5. The spectra of SBA-15 show specific bands at 460, 802, 1086 and 1634 cm^{-1}, which are attributed to Si–O–Si bands (Fig. 5a), the condensed network of mesoporous silica. A very broad band at 3447 cm^{-1} ascribed to silanol stretching vibration and OH group of water molecules present into the

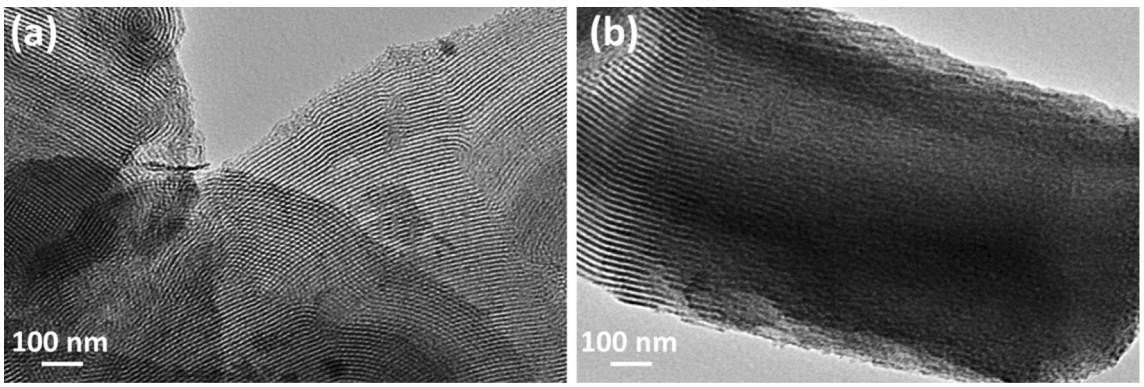

Fig. 3 HRTEM images of **a** SBA-15 and **b** saponin-loaded SBA-15

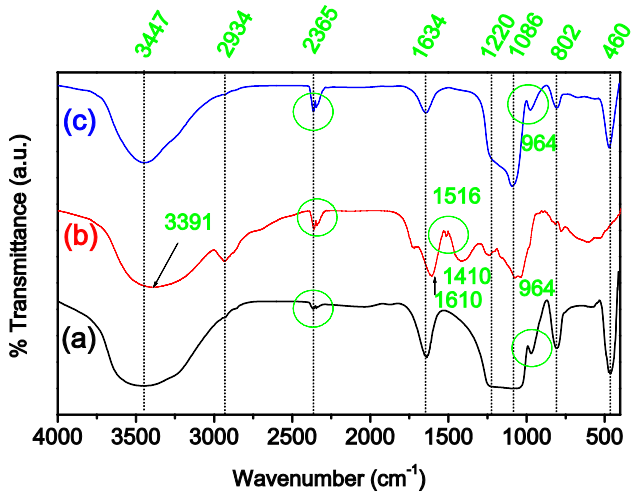

Fig. 5 FTIR spectra of (a) SBA-15, (b) saponin and (c) saponin-loaded SBA-15

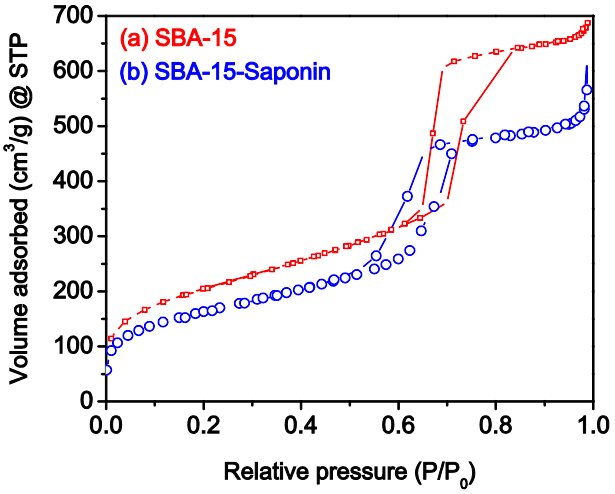

Fig. 6 N_2 adsorption–desorption isotherms of (a) SBA-15 and (b) saponin-loaded SBA-15

mesoporous structure of SBA-15 [16]. A band at 1086 cm^{-1} corresponds to Si–O asymmetric stretching [29]. Any weak peaks in the range 940–965 cm^{-1} ascribed to non-condensed Si–OH groups [30]. Also, the silanol groups of mesoporous SBA-15 shows a weak peak at 964 cm^{-1}. The FTIR spectra of saponin show typical bands at 2365, 2934 and 3391 cm^{1} with various bands such as 1610, 1516, 1410, 1220 and 1086 cm^{-1} in the fingerprint region (Fig. 5b) [30]. The FTIR spectra of saponin-loaded SBA-15 show the significant variation in two bands such as 2365 and 1220 cm^{-1} (Fig. 5c). The variation in these bands may be considered as proof for loading of saponin into SBA-15 mesoporous structure. In case of saponin-loaded SBA-15, the infrared band located at 460 cm^{1} corresponds to T–O bend vibration [16] and the band located at 1086 cm^{-1} corresponds to T–O4 asymmetrical vibration of Si–O–Si [21]. The existence of these infrared bands specifies that the saponin loading into SBA-15 does not destroy its main structure.

3.6 Saponin loading studies

To estimate the concentration of saponin in saponin-loaded SBA-15, the spectrophotometry was used [21]. The estimated saponin loading efficiency (P_E) into SBA-15 was 85%. Nitrogen (N_2) adsorption–desorption curves are very effective in determining the surface properties of mesoporous materials including surface area, pore volume and pore size distribution. The adsorption–desorption isotherms and BJH pore size distributions curves of SBA-15 and saponin-loaded SBA-15 are shown in Figs. 6 and 7 respectively. Both the pristine SBA-15 and loaded SBA-15 exhibit a typical irreversible type IV isotherm along with H1-type hysteresis loop. Such type of isotherm with hysteresis loop is a characteristic of porous material having hexagonal cylindrical channels with open pores [31, 32]. In case of saponin-loaded SBA-15, the quantity of nitrogen uptake falls due to the shrinkage of mesopore volume (Fig. 6). The shrinkage of volume also leads to the decrease in size of mesopores as shown by corresponding pore size distribution curve (Fig. 7). The pristine SBA-15 reveals the specific surface area of ~737 m^2/g with pore volume ~0.94 cm^3/g and pore diameter ~9.4 nm. All these three parameters decreased due to saponin loading in mesoporous silica. The saponin-loaded SBA-15 shows the specific surface area of ~585 m^2/g with pore volume ~0.84 cm^3/g and pore diameter ~7.3 nm. The N_2 adsorption–desorption isotherms of saponin-loaded SBA-15 reveals that the basic mesoporous structure as well as pore shape of SBA-15 remain unaffected, which signifies

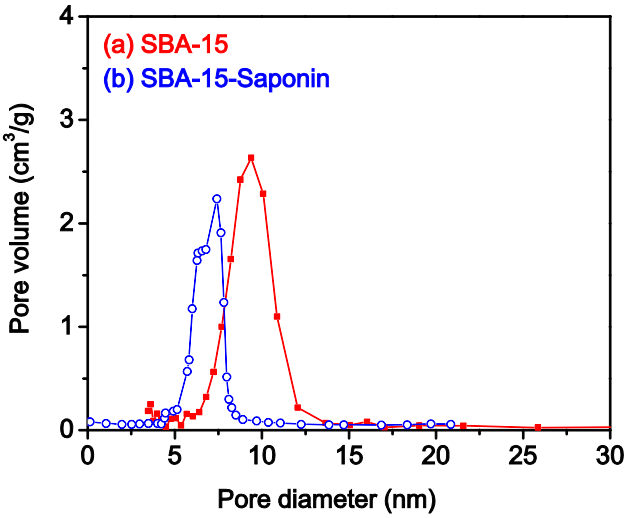

Fig. 7 BJH pore size distribution curves of (a) SBA-15 and (b) saponin-loaded SBA-15

that the saponin molecules are loaded into the mesochannels of SBA-15 without pore plugging.

3.7 In vitro saponin release studies

The saponin loading efficiency (P_E) of SBA-15 was found to be 85%. In vitro release of saponin was measured with PBS (pH 7.4). The release % of saponin from mesoporous SBA-15 at predefined time intervals was determined using Eq. (3). Figure 8 demonstrates the in vitro release profile of saponin. The saponin is showing a fast initial drug release rate that can be designated as the "burst release". Over the time range of 0.25–12 h, the constant release rate of saponin accelerated and a released amount of 65.4% was achieved. After 12 h, a relatively slow release rate was observed till 72 h and 80.3% of the saponin was released. An initial burst release was expected because of the saponin molecules attached onto the surface of SBA-15 particles. However, the constant and slow release was due to the entrapped saponin. The saponin release occurred due to diffusion of drug from pores of SBA-15. The declined release rate of saponin at longer time recommended the significance of the diffusion in release kinetics [33]. The measured slow and constant release of saponin after initial burst release is noteworthy because controlled drug release is obligatory in cancer therapy. These results specified that the saponin-loaded SBA-15 is a beneficial controlled drug delivery system especially for cancer treatment.

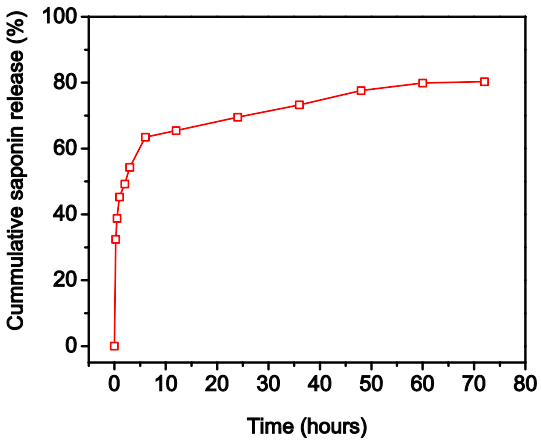

Fig. 8 In vitro release profile of saponin from saponin-loaded SBA-15

3.8 Cytotoxicity studies

An in-vitro anticancer activity of saponin-loaded SBA-15 was studied against Panc-I cells. Figure 9a shows the control Panc-I cell free from any drug and SBA-15 nanoparticles, while Fig. 9b displays a completely damaged Panc-I cell after treatment with saponin-loaded SBA-15. Both the SBA-15 and saponin-loaded SBA-15 has the potential to damage the Panc-I cell within 48 h. The saponin-loaded SBA-15 damaged the nucleus of Panc-I cancer cell. Due to the destruction of nucleus of the cancer cell, there is no chance of redevelopment of that cell. After the treatment with nanosaponin, cancer cell lost its apoptosis and melgnant property.

The toxicity of SBA-15 was analyzed by MTT on Panc-I cancer cells. The SBA-15 nanoparticles were found toxic on Panc-I cells (Fig. 10). However, the nanosaponin presented precise toxicity on cancer cells (Fig. 10).

Generally, saponins isolated from various plants and animals precisely prevent the evolution of in vitro cancer cells [34–39]. The ability of natural substances to control malignancies led to extensive research on this typical property of saponins. The saponin extracted from Gymnemasylvestre leaves show toxicity on Hela cells (human cervical carcinoma) [40]. Similarly, the saponins extracted from *Paris polyphylla* var. yunnanensis show toxicity to tumor

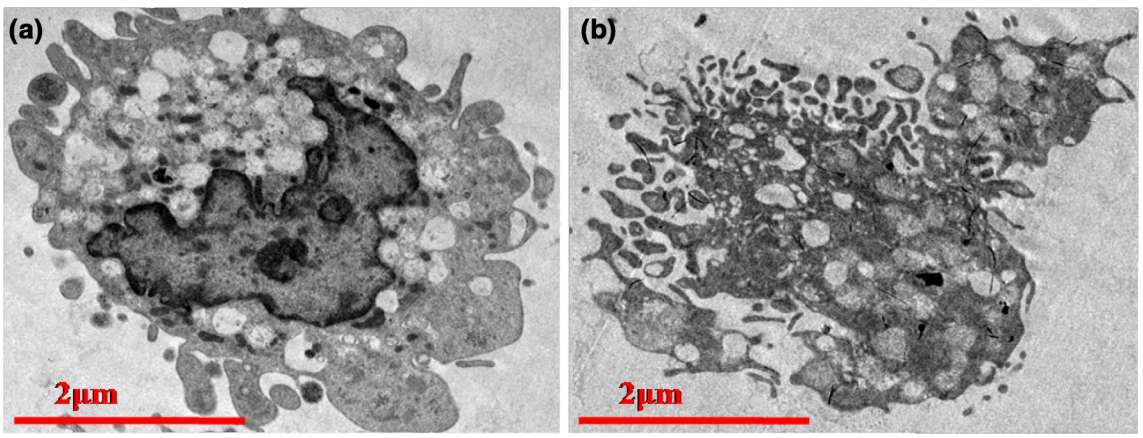

Fig. 9 TEM images of **a** untreated Panc-I cancer cell and **b** damaged Panc-I cancer cell after treatment with saponin-loaded SBA-15

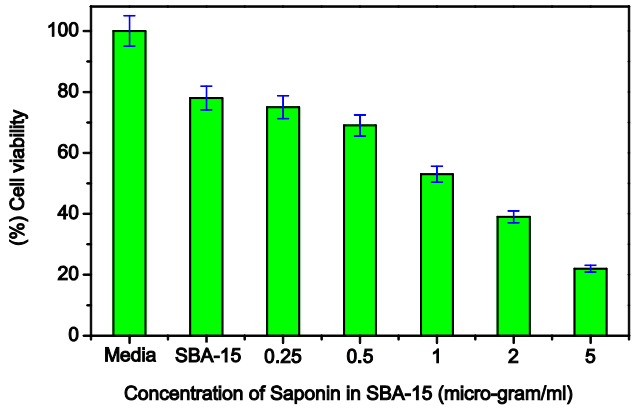

Fig. 10 MTT assay of SBA-15 and saponin-loaded SBA-15 on Panc-I cancer cells

cells [41]. This indicates that some molecular level mechanism happening for saponin to present particular toxicity on cancer cells. Therefore, additional studies on this characteristic are highly desired to develop better understanding on detailed anticancer action of the saponins. The toxic action of saponins on various cancer cells can happen via numerous and complex mechanisms. The discriminatory restriction on tumor growth has been identified using triterpenoid saponins. That happened by cell cycle arrest in human breast cancer cells as well as apoptosis in leukaemia cells [42]. Saponins based on the structural functionalities can prompt a cell cycle arrest facilitated by restriction of the phosphatidylinositol-3-kinase–protein kinase signaling pathway [42] or uninterrupted destruction of protein kinase complex genes [43].

In the present study, saponin-loaded SBA-15 can induce Panc-I cancer cell death, which is an interesting observation. However, apoptosis is a process of tissue homeostasis and can be considered as an ideal pathway to restrict cancer cell growth. This study is focused on the anticancer activity of saponin-loaded SBA-15, which is clearly revealing that a constant saponin release rate could be possible to cancer cells. The saponin alone can totally expire once triggering sudden death to a certain population of cancer cells [3]. But, the saponin-loaded SBA-15 can release the saponin in a controlled manner to cause toxicity to those cancer cells for long time.

4 Conclusions

Mesoporous silica, SBA-15 was synthesized and used to load saponin drug. First time, saponin was successfully introduced into the mesoporous channels of SBA-15. Maximum loading efficiency of 85% was achieved. Small-angle XRD and electron microscopy confirmed the homogeneous dispersion of saponin into the pores of SBA-15. FTIR spectra and N_2 adsorption–desorption isotherms revealed no structural change in mesoporous channel structure of SBA-15 due to saponin loading and also verified the successful encapsulation of saponin into the mesochannels of SBA-15. FTIR studies also indicated the possibility of some interaction of saponin with the SBA-15. After initial burst release, a sustained release of saponin was observed up to 72 h with a maximum release of 80.3%. The SBA-15 showed specific toxicity on Panc-I cancer cells. However, saponin-loaded SBA-15 revealed significant toxicity on the cancer cells. This study presented sufficient evidence of nanotechnology based saponin in vitro delivery to Panc-I cancer cell to improve the therapeutic efficiency of this well-known green chemotherapeutic agent.

References

1. S. Man, W. Gao, Y. Zhang, L. Huang, C. Liu, Fitoterapia **81**, 703 (2010)
2. S.G. Sparg, M.E. Light, J. van Staden, J. Ethnopharmacol. **94**, 219 (2004)
3. N.S. Rejinold, M. Muthunarayanan, K. Muthuchelian, K.P. Chennazhi, S.V. Nair, R. Jayakumar, Carbohydr. Polym. **84**, 407 (2011)
4. C.R. Kensil, U. Patel, M. Lennick, D. Marciani, J. Immunol. **146**, 431–437 (1991)
5. J.B. Campbell, Y.A. Peerbaye, Res. Immunol. **143**, 526 (1992)
6. D.J. McWeeny, Food Chem. Toxicol. **31**, 149 (1993)
7. I.E. Liener, Proc. Nutr. Soc **29**, 56 (1970)
8. H. Chen, J.N. Seiber, M. Hotze, J. Agric. Food Chem **62**, 1209 (2014)
9. J. Du, X. Li, H. Zhao, Y. Zhou, L. Wang, S. Tian, Y. Wang, Int. J. Pharm. **495**, 738 (2015)
10. B.E. Rabinow, Nat. Rev. Drug Discov. **3**, 785 (2004)
11. M. Kakran, R. Shegokar, N.G. Sahoo, S. Gohla, L. Li, R.H. Müller, J. Pharm. Pharmacol. **64**, 1394 (2012)
12. Z.H. Loh, A.K. Samanta, P.W. Sia, Heng, Asian J. Pharm. Sci. **10**, 255 (2015)
13. D. Zhao, Q. Huo, J. Feng, B.F. Chmelka, G.D. Stucky, J. Am. Chem. Soc. **120**, 6024 (1998)
14. S. Che, A.E. Garcia-Bennett, T. Yokoi, K. Sakamoto, H. Kunieda, O. Terasaki, T. Tatsumi, Nat. Mater. **2**, 801 (2003)
15. S. Jangra, P. Girotra, V. Chhokar, V.K. Tomer, A.K. Sharma, S. Duhan, J. Porous Mater. **23**, 679 (2016)
16. S. Jangra, V. Chhokar, V.K. Tomer, A.K. Sharma, S. Duhan, J. Porous Mater. (2016). doi:10.1007/s10934-016-0162-7
17. V.K. Tomer, R. Malik, S. Jangra, S.P. Nehra, S. Duhan, Mater. Lett. **132**, 228 (2014)
18. M. Van Speybroeck, V. Barillaro, T. Do Thi, R. Mellaerts, J. Martens, J. Van Humbeeck, J. Vermant, P. Annaert, G. Van den Mooter, P. Augustijns, J. Pharm. Sci. **98**, 2648 (2009)
19. M. Thanou, J.C. Verhoef, H.E. Junginger, Adv. Drug Deliv. Rev. **52**, 117 (2001)
20. K.A. Fisher, K.D. Huddersman, M.J. Taylor, Chemistry **9**, 5873 (2003)
21. Q.-Z. Zhai, Mater. Sci. Eng. C **32**, 2411 (2012)
22. V. Ambrogi, L. Perioli, C. Pagano, F. Marmottini, M. Ricci, A. Sagnella, C. Rossi, Eur. J. Pharm. Sci. **46**, 43 (2012)
23. S.-C. Shen, W.K. Ng, L. Chia, J. Hu, R.B.H. Tan, Int. J. Pharm. **410**, 188 (2011)

24. M. Kruk, M. Jaroniec, C.H. Ko, R. Ryoo, Chem. Mater. **12**, 1961 (2000)
25. V. Meynen, P. Cool, E.F. Vansant, Microporous Mesoporous Mater. **125**, 170 (2009)
26. W.-H. Zhang, J.-L. Shi, H.-R. Chen, Z.-L. Hua, D.-S. Yan, Chem. Mater. **13**, 648 (2001)
27. N. Gargiulo, D. Caputo, C. Colella, *From Zeolites to Porous MOF Materials—The 40th Anniversary of International Zeolite Conference, Proceedings of the 15th International Zeolite Conference*, (Elsevier, 2007)
28. A. Katiyar, S. Yadav, P.G. Smirniotis, N.G. Pinto, J. Chromatogr. A **1122**, 13 (2006)
29. N. Navascués, C. Téllez, J. Coronas, Microporous Mesoporous Mater. **112**, 561 (2008)
30. H. Wang, X. Gao, Y. Wang, J. Wang, X. Niu, X. Deng, Ceram. Int. **38**, 6931 (2012)
31. D. Zhao, J. Sun, Q. Li, G.D. Stucky, Chem. Mater. **12**, 275 (2000)
32. G. Leofanti, M. Padovan, G. Tozzola, B. Venturelli, Catal. Today **41**, 207 (1998)
33. A. Dev, J.C. Mohan, V. Sreeja, H. Tamura, G.R. Patzke, F. Hussain, S. Weyeneth, S.V. Nair, R. Jayakumar, Carbohydr. Polym. **79**, 1073 (2010)
34. T. Konoshima, M. Takasaki, H. Tokuda, H. Nishino, N.M. Duc, R. Kasai, K. Yamasaki, Biol. Pharm. Bull. **21**, 834 (1998)
35. T.A. Kuznetsova, M.M. Anisimov, A.M. Popov, S.I. Baranova, S.S. Afiyatullov, I.I. Kapustina, A.S. Antonov, G.B. Elyakov, Comp. Biochem. Physiol. C **73**, 41 (1982)
36. S. De Marino, M. Iorizzi, E. Palagiano, F. Zollo, C. Roussakis, J. Nat. Prod. **61**, 1319 (1998)
37. Y. Mimaki, M. Kuroda, A. Kameyama, A. Yokosuka, Y. Sashida, Phytochemistry **48**, 1361 (1998)
38. I. Podolak, M. Elas, K. Cieszka, Phyther. Res. **12**, S70 (1998)
39. A.V. Rao, M.K. Sung, J. Nutr. **125**, 717S (1995)
40. V.G. Khanna, K. Kannabiran, Int. J. Green Pharm. **3**, 227 (2009)
41. L.L. Yan, Y.J. Zhang, W.Y. Gao, S.L. Man, Y. Wang, Exp. Oncol. **31**, 27 (2009)
42. K. Mujoo, V. Haridas, J.J. Hoffmann, G.A. Wächter, L.K. Hutter, Y. Lu, M.E. Blake, G.S. Jayatilake, D. Bailey, G.B. Mills, J.U. Gutterman, Cancer Res. **61**, 5486 (2001)
43. W.K. Liu, S.X. Xu, C.T. Che, Life Sci. **67**, 1297 (2000)